





RESEARCH ARTICLE | MARCH 06 2024

Long-range, water-mediated interaction between a moderately active antifreeze protein molecule and the surface of ice

Joanna Grabowska ; Anna Kuffel ; Jan Zielkiewicz  

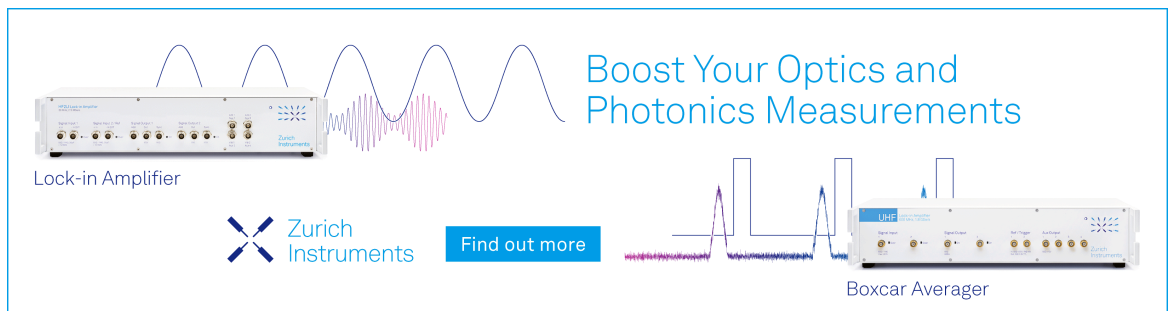


J. Chem. Phys. 160, 095101 (2024)

<https://doi.org/10.1063/5.0187663>




CrossMark



Boost Your Optics and Photonics Measurements

Lock-in Amplifier

 Zurich Instruments

[Find out more](#)

Boxcar Averager

Long-range, water-mediated interaction between a moderately active antifreeze protein molecule and the surface of ice

Cite as: *J. Chem. Phys.* **160**, 095101 (2024); doi: [10.1063/5.0187663](https://doi.org/10.1063/5.0187663)

Submitted: 15 November 2023 • Accepted: 16 February 2024 •

Published Online: 6 March 2024



View Online



Export Citation



CrossMark

Joanna Grabowska,^{a)}  Anna Kuffel,^{b)}  and Jan Zielkiewicz^{c)} 

AFFILIATIONS

Faculty of Chemistry, Department of Physical Chemistry, Gdańsk University of Technology, Narutowicza 11/12, 80-233 Gdańsk, Poland

^{a)}Electronic mail: joanna.grabowska@pg.edu.pl

^{b)}Electronic mail: anna.kuffel@pg.edu.pl

^{c)}Author to whom correspondence should be addressed: jan.zielkiewicz@pg.edu.pl

ABSTRACT

Using molecular dynamics simulations, we show that a molecule of moderately active antifreeze protein (type III AFP, QAE HPLC-12 isoform) is able to interact with ice in an indirect manner. This interaction occurs between the ice binding site (IBS) of the AFP III molecule and the surface of ice, and it is mediated by liquid water, which separates these surfaces. As a result, the AFP III molecule positions itself at a specific orientation and distance relative to the surface of ice, which enables the effective binding (via hydrogen bonds) of the molecule with the nascent ice surface. Our results show that the final adsorption of the AFP III molecule on the surface of ice is not achieved by chaotic diffusion movements, but it is preceded by a remote, water-mediated interaction between the IBS and the surface of ice. The key factor that determines the existence of this interaction is the ability of water molecules to spontaneously form large, high-volume aggregates that can be anchored to both the IBS of the AFP molecule and the surface of ice. The results presented in this work for AFP III are in full agreement with the ones obtained by us previously for hyperactive CfAFP, which indicates that the mechanism of the remote interaction of these molecules with ice remains unchanged despite significant differences in the molecular structure of their ice binding sites. For that reason, we can expect that also other types of AFPs interact with the ice surface according to an analogous mechanism.

Published under an exclusive license by AIP Publishing. <https://doi.org/10.1063/5.0187663>

I. INTRODUCTION

The functioning of antifreeze proteins (AFPs), since their discovery more than half a century ago, has been of great interest among researchers. The general mechanism of action of AFPs refers to the Gibbs–Thomson phenomenon, predicting a decrease in the freezing point of a convex ice surface. This mechanism, which assumes the permanent adsorption^{1–3} of AFP molecules onto the ice surface, is widely accepted, although the details of the adsorption process are still unclear. In particular, it is disputed how an AFP molecule, being surrounded by liquid water, recognizes the ice surface. The process of binding of an AFP onto the ice is enabled by the specific structure of the active region on its surface (ice-binding surface, or IBS): both the flat shape and the way hydrophilic

and hydrophobic groups are arranged on this surface turn out to be important in giving this area an affinity for ice.⁴ This affinity strongly suggests the presence of a characteristic “ice-like” solvation pattern of the IBS, which has been observed by many authors.^{5–9} This kind of ice-like structure of solvation water was also observed in the solid phase by Garnham *et al.*:¹⁰ the authors, based on x-ray crystallographic images of the interaction of an *MpAFP* molecule with water molecules at 100 K, have proposed the concept of “anchored clathrate water” (ACW). According to this idea, anchored clathrate water molecules bind to the IBS of the protein, adopting positions that will then allow them to fit into the crystal lattice of ice. Thus, to some extent, the AFP molecule bears its own “ice”¹¹ in the form of structured, ice-like water layer that is anchored to the protein’s surface. The arrangement of water molecules consistent with the ACW

model was also observed by other authors in the solvation water of *LpAFP*¹² and *TisAFP*.¹³ Note that while the ACW concept seems intuitive and reasonable, there is controversy about the significance of the role that the ordering of the clathrate-anchored aqueous layer plays in the AFP mechanism of action.^{14,15}

As we have shown previously,^{16–18} the process of adsorption begins when the AFP molecule approaches the surface of ice. The reason for this is that the ice–liquid water interface is not sharp: the thickness of the transition region is equal to about 1 nm^{19–22} and depends on the temperature. In addition, the extent of the solvation shell of proteins is typically assumed to be of the same order.^{23,24} Therefore, there is an overlap between the two solvation shells and the interaction of the solvation water of an AFP with the solvation water of ice, which occurs even before the protein molecule contacts the ice itself, is what determines the early stages of the adsorption process.

The model describing this interaction refers to the unusual properties of liquid water that distinguish it from other molecular liquids. In 2000, Tanaka²⁵ published a model describing the structure of liquid water, which assumes that there are two types of structural ordering in it, characterized by two independent order parameters. The first type is translational ordering, tending toward the tightest possible spatial packing of molecules in the liquid; a measure of this ordering is the density of the liquid. The second type is orientational ordering, resulting from the directional properties of hydrogen bonds. This ordering manifests itself in a tendency to maintain both a certain preferred spatial arrangement and a mutual orientation of the water molecules; the latter tendency, building spatially ordered structures with a significant volume of their own, naturally opposes the increase in the density. While describing his model Tanaka assumed, as Nemethy and Scheraga did at one time,²⁶ that energetically stable “locally favored structures” (LFSs) characterized by a significant intrinsic volume are formed in liquid water—they are aggregates built by water molecules connected by hydrogen bonds. They exist in the liquid water in a relatively small amount, while remaining surrounded by a “sea” of disordered water molecules, forming a phase of above-average density. The parameter describing the degree of orientational ordering of water is, according to Tanaka, simply the content of these aggregates formed in liquid water. Thus, a specific pressure- and temperature-dependent equilibrium is established in liquid water, determining the relative content of the two structural forms (i.e., ordered and disordered). The position of this equilibrium determines the values of various physicochemical parameters of water, such as density, viscosity, and compressibility, while explaining the occurrence of known thermodynamic anomalies (e.g., the occurrence of a maximum of density of water at 4 °C).²⁷

Some of the locally favored structures considered by Tanaka are consistent with the structure of hexagonal ice and appear in increasing amount during the solidification process.^{27,28,32} As examples of such structures, hexagonal rings or the so-called octameric units built by interconnected hexagonal rings can be given.^{28,29} Other LFSs may not be consistent with the structure of hexagonal ice, for example 5-membered rings (also nearly stress-free), whose presence in the liquid phase is responsible for the ability of liquid water to transition to a glassy state.^{30,31}

According to Tanaka’s model, locally favored structures are well-defined (of highly ordered geometry), unique, and local (the

order is short-range).²⁵ In our work, we would like to draw from Tanaka’s model but without applying strict geometric criteria for the ordered structures. We will simply be looking for hydrogen-bonded aggregates of water molecules that are characterized by a relatively high volume. By definition, these aggregates do not have to have an exact geometry of the building blocks of hexagonal ice (or LFSs) or have a specific size, but it can be expected that they will be built by small low-energy building blocks, such as 5- and 6-membered rings of hydrogen-bonded water molecules. To distinguish them from the LFSs, we will refer to them as high volume aggregates (HVAs), as previously proposed¹⁵ (see also the discussion included in the cited reference).

In this work, we employ the concepts presented above to propose a model of interaction of the IBS of an AFP molecule and the surface of ice. We begin by postulating that in the solvation water of a solute, the position of the above-mentioned equilibrium (between high and low density local structures) depends on the character of the interactions between the liquid water and the surface of the solute molecule (e.g., protein). Depending on the geometry and the chemical nature of the hydrated surface, HVAs undergo either destruction or additional stabilization due to interactions with this surface. This is how we explained the well-known phenomenon of an increase in the density of solvation water of proteins;³³ we have shown that in the vicinity of the surface of a protein molecule, HVAs are destroyed, resulting in the increase in density (compared to bulk water). This effect occurs for most proteins; however, in the vicinity of the IBS of AFP molecules, the balance between the two structural forms of water is shifted in the other direction, enhancing the tendency to form HVAs.¹⁵ Since the process of water freezing proceeds through a gradual remodeling of the structure of the liquid in the direction of HVAs’ formation and merging,^{28,32} it can be said that the HVAs “anchored” to the IBS form a kind of crystallization nuclei for the solid phase. In the case of AFPs, these nuclei are subcritical; hence, the molecules of AFPs do not facilitate the nucleation of ice (however, it has been shown that in some cases, AFPs can trigger ice nucleation³⁴). Increasing the number and/or size of HVAs in the vicinity of the IBS facilitates the transformation of liquid water into a solid phase, while their anchoring to the IBS is responsible for the final adsorption of the AFP molecule onto the ice. This is a direct relation to the ACW concept mentioned above.

It is worth noting here that the initial recognition and interaction of AFPs with the surface of ice do not necessarily guarantee their binding to ice. Recent studies^{35,36} have shown that even molecules of proteins that have no antifreeze activity (non-AFPs) are able to slow down the growth of ice and in some cases bind with its surface. The authors also showed that if a molecule of non-AFP is artificially kept close to the surface of ice, it can stop the growth of ice completely. It is direct evidence that the irreversible binding of protein onto the surface of ice is crucial for the antifreeze activity, regardless of the way in which the binding was accomplished. In addition, Voets *et al.*³⁷ have shown in an experimental study that a moderately active type III AFP binds irreversibly with ice, while the non-active mutant of this protein binds with ice reversibly. This clearly demonstrates that the non-active variants of AFPs can still be able to interact with the ice surface, but the inability to bind irreversibly to the ice prevents them from stopping the growth of ice.

In order to confirm the role of HVAs in the recognition and interaction of AFPs with ice, it is necessary to both confirm the existence of HVAs in the solvation water of IBSs of AFPs and show that the structural changes in the intermediate (i.e., contained between the IBS and the ice crystal) layer of water go in the direction of increasing HVA content as the time progresses. Our aim is to provide a description of the process of the recognition of ice by AFPs at initial stages of their adsorption onto the ice. This has already been partially done in our previous work,¹⁸ with regard to the hyperactive CfAFP. However, in the case of the hyperactive protein, just because of its high activity, the observed solvation effects are very distinct and perhaps not representative of all AFPs. Therefore, we have chosen a protein with a moderate activity—type III AFP from the ocean pout *Macrozoarces americanus*, in this paper denoted as AFP III. The molecule of this protein is relatively small (~7 kDa) and has a much smaller IBS compared to the hyperactive CfAFP. Moreover, the chemical structure of their IBSs is different: the ordered matrix of threonine residues (THR), so characteristic for hyperactive proteins, is absent in the case of AFP III. In our opinion, demonstration of the validity of the model for both CfAFP and AFP III can serve as a basis for making generalizations and postulating its correctness for other AFPs.

II. METHODS

A. System setup

The results were obtained with the use of molecular dynamics. We conducted computer simulations using the Amber16³⁸ package and the ff03 force field, under NpT conditions. The temperatures were kept constant by a Berendsen thermostat.³⁹ The pressure of 1 bar was kept constant using the weak coupling method. The lengths of the bonds involving hydrogen atoms were fixed using the SHAKE procedure. The cutoff for nonbonding interactions was equal to 1.2 nm. The equations of motion were integrated with a time step of 2 fs. Periodic boundary conditions were applied for the simulation boxes in all three dimensions. In all simulation systems, TIP4P/Ice⁴⁰ model of water was used, as its melting temperature (270 K⁴¹) is close to the experimental value.

B. Simulation procedure

For our study, we have chosen the molecule of type III AFP (QAE HPLC-12 isoform, denoted in this work as AFP III), derived from the *Macrozoarces americanus* (eelpout). The starting structure of the molecule was taken from the Protein Data Bank (PDB code 1MSI⁴²). We adjusted this structure to match the native form of the isoform HPLC-12⁴³ by changing the second alanine in the amino acid sequence to asparagine. In some simulations, we have also used a mutant of this protein where one of the threonines in the IBS was replaced by asparagine (T18N, PDB code 9MSI). This mutation causes the protein molecule to lose most of its antifreeze activity.⁴⁴

As a measure of “antifreeze activity,” the width of the hysteresis gap is commonly used (which is the difference between the melting point and the freezing point of water in the presence of a cryoprotectant). For example, for AFP III, it was reported that the width of the hysteresis gap is 0.23 °C at a protein concentration of 1 mg/ml,^{45,46} while for the hyperactive insect protein, *TmAFP*, the width of the

gap is 5.5 °C at the same protein concentration.⁴⁷ Since the AFP III molecule studied here has a relatively low activity (which is typical for this class of AFPs), it is appropriate to study the behavior of the system at a relatively low degree of supercooling. For that reason, we conducted simulations at 270 K.

Following the procedure proposed by Kuiper *et al.*,⁴⁸ for our simulation systems, we prepared a slab of ice inclined at a slight angle and located in a cuboidal simulation box. The slab inclination angle was chosen so that the new layer of ice formed on its surface would maintain continuity with its image resulting from the periodic environment. This procedure significantly facilitates the process of building up successive layers of ice on the surface of the slab.

Three types of systems were prepared: where the molecule of a native AFP III was facing the primary prism (10 $\bar{1}$ 0) plane of the ice slab with its IBS, where the molecule of a mutant of AFP III (T18N) was facing the primary prism plane of the ice slab with its IBS, and where the molecule of a native AFP III was facing the primary prism plane of the ice slab with its non-IBS. In all cases, the molecule of the protein was placed at a short distance of about 1 nm from the ice surface [see Fig. 1(a)]. The simulation boxes contained over 15 000 molecules of water each, and their sizes were equal to about 8.0 × 8.5 × 7.0 nm³.

The IBS of AFP III has been identified before in the mutagenesis studies.^{44,49} Within the IBS, two areas can be distinguished,⁵⁰ positioned at an angle of 150° relative to each other—one is responsible for binding with a primary prism plane of ice, while the other is responsible for binding with a pyramidal plane of ice. In addition, within the IBS, five atoms capable of forming hydrogen bonds with water molecules and considered essential in the process of binding of the AFP III molecule with the surface of ice can be distinguished:⁴⁴ NE2 atom of GLN9, OG1 atom of THR15, O atom of ALA16, OG1 atom of THR18 (or ND2 of ASN18 in the case of a mutated protein), and NE2 atom of GLN44. In our simulation systems, the molecule of AFP III (or its mutant) was placed in the simulation systems in such a way that the relatively flat area of IBS, within which these five atoms are located, was facing the surface of the ice slab.

All the prepared systems were copied 100 times each, and in each copy, the orientation of the protein molecule in relation to the surface of ice was randomized (each protein molecule has been rotated by a random angle around the axis passing through its center

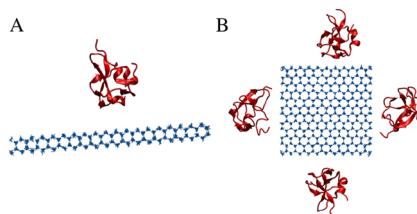


FIG. 1. A visualization of the simulated systems. (a) System consisting of an inclined ice slab and the AFP III molecule located at a distance from the surface (the primary prism plane) of the slab. In this figure, the system where the AFP III molecule is facing the ice with its IBS is shown. (b) System consisting of a cuboidal ice crystal and four molecules of AFP III neighboring faces of the crystal. The crystal faces are basal, primary prism and secondary prism planes of ice. The picture was generated in VMD.⁵¹

of mass and perpendicular to the surface of the ice slab and translated in the random direction parallel to the surface of the ice slab by a random distance in the range of ± 0.25 nm). The systems were then solvated with the use of the TIP4P/Ice water model. In the next step, the orientations of all water molecules building the ice slabs were randomized.

The systems were then minimized and equilibrated in two steps. The first equilibration was conducted at a temperature of 300 K under NpT conditions, for 1 ns. In the second one, the temperature was lowered to 280 K. These simulations were carried out for 3 ns. The equilibration time was inevitably limited, since we wanted the solidification process not to be very advanced at the beginning of the actual simulations. We consider the chosen value (3 ns) to be sufficient, since the dynamics of water is relatively fast (compared, for example, with the dynamics of conformational changes of a protein molecule).

During all the above-mentioned simulations, the oxygen atoms of the water molecules building the ice slab and the atoms of the protein backbone were restrained at the reference coordinates with the use of the harmonic potential (in the first step of the equilibration process, the value of the force constant equal to $50 \text{ kcal}/(\text{mol } \text{Å}^2)$ was used, while for the second step, the values of 2 and $0.02 \text{ kcal}/(\text{mol } \text{Å}^2)$ were used for oxygen atoms of the water molecules in the ice slab and backbone atoms of the protein molecule, respectively).

The production simulations were conducted under NpT conditions, at 270 K. The positions of the protein backbone atoms were no longer restrained. The length of each of the 100 simulations carried out for the three types of systems prepared was equal to 35 ns.

In addition, following the procedure described above, we carried out simulations of the systems that consisted of only the ice slab and liquid water. In these systems, the surface of the slab was the primary prism plane of ice. The simulations were conducted at a temperature of 270 K.

Since our previous work¹⁸ on the CfAFP was carried out at a temperature of 250 K, some of the calculations for AFP III were additionally carried out at a temperature of 250 K, to compare the results currently obtained with those obtained for CfAFP. The systems were constructed in a way matching our CfAFP study—each system consisted of a cuboidal ice crystal with an edge length of ~ 4.5 nm and four molecules of AFP III located at different distances from the crystal walls [Fig. 1(b)]. We prepared 360 independent systems, in which the molecules of AFP III were facing the primary prism plane of ice with the IBS and the secondary prism plane of ice with the non-IBS. Since in every system there were two molecules of protein facing the same crystallographic plane of ice, we obtained 720 independent configurations for both types of systems. The details of the simulation procedure can be found in our paper regarding CfAFP.¹⁸ The production runs were carried out at 250 K for 12 ns each. Since one of the aims of these simulations was to measure the force⁵² exerted by the growing ice on the protein molecules, one atom in each protein molecule was held in the reference position during simulations with the use of a harmonic potential [$k = 10 \text{ kJ}/(\text{mol } \text{Å}^2)$].

We studied the structural properties of the solvation water of the IBS region of the AFP molecule in a 0.4 nm thick layer (the same as in our previous work;¹⁸ this is approximately the position of the first minimum on the curve representing the distribution of water density as a function of distance from the surface of the protein

molecule). The analysis was conducted using the order parameter p and the number of rings formed by water molecules connected by hydrogen bonds.

C. Order parameter p

A rational measure of the degree of order is the entropy of the system. The order parameter p is defined⁵³ on the basis of theoretical considerations of the way statistical entropy can be calculated. The starting point is the expansion of the expression for the entropy of a system composed of N particles into a series depending on the n -particle ($n = 1, 2, \dots, N$) correlation functions, which was given by Green.⁵⁴ Restricting this series to the term describing two-particle interactions provides an approximate formula for the statistical entropy of the system. This term, which is the (dominant) two-particle contribution to the entropy of the system, is given by the integral of an expression containing the two-particle correlation function, g^2 , as described in the cited article. The value of this integral is calculated in the area encompassing the closest surroundings of the central water molecule; the boundary of this immediate neighborhood is the extent of the second hydration shell around the analyzed molecule, equal to 0.58 nm. Moreover, we have shown before⁵³ that this parameter can be represented as a sum of three terms,

$$p = p_{tra} + p_{con} + p_{ort},$$

where the individual components p_{tra} , p_{con} , and p_{ort} reflect the contributions derived from the translational order (p_{tra} , depending only on the distance between the molecules) and the orientational order (p_{con} and p_{ort} , characterizing the mutual orientation of two adjacent water molecules). The values of the p_{con} and p_{ort} parameters are proportional to each other,^{23,53} so it is possible to use only the p_{con} parameter instead of the sum of $p_{con} + p_{ort}$; this allows for a significant simplification of the calculation procedures. As it results from the definition, the values of the p_{tra} and p_{con} parameters are always non-positive: equal to zero in a state of a complete disorder (for an ideal gas), and as the degree of order increases, their values become increasingly negative. The benefit of such a decomposition of the p -parameter into the sum of two components is that it allows for a deeper investigation of the structural changes occurring in water near the point of phase transition.⁵⁵

The values of the two-particle water–water correlation function (g^2) in a binary system containing water and a solute are affected by two factors. The first is the “excluded volume” effect, caused by the presence of the protein molecule; this effect strongly depends on both the size and the shape of the solvated surface. The second factor is the modification of the way that water molecules are arranged in the solvation layer of the protein molecule (with respect to the arrangement characteristic for bulk water).²³ Since we are only interested in the latter effect, in order to eliminate the “excluded volume” factor, we created a fictitious “reference” system by filling the solvation layer of the protein molecule with bulk water. Thus, determining the values of the parameters $(p_{tra})_{bulk}$ and $(p_{con})_{bulk}$ in the so-defined fictitious system gives us a point of reference, while the calculated differences in p -parameter values in both systems: $\Delta p_{tra} = (p_{tra})_{solv} - (p_{tra})_{bulk}$ and $\Delta p_{con} = (p_{con})_{solv} - (p_{con})_{bulk}$, reflect the change in the structure of solvation water resulting from its specific interactions with the solvated surface. The values of Δp_{tra} and

Δp_{con} obtained in this way determine the position of the point on the ordering map.

However, this analysis does not give us any detailed information about the spatial arrangement and mutual orientation of the water molecules; it is, therefore, difficult to conclude whether and to what extent this ordering is “ice-like.” To resolve this, we performed analogous calculations also for the solvation water of ice crystal, since in this case the direction of the structural changes that take place during freezing is known. A comparison of the time-dependent changes in the position of points on the ordering map, representing the state of the solvation water of the protein molecule and the state of the solvation water of ice, allows us to draw conclusions regarding similarities and differences between them.

D. 5- and 6-membered rings and the τ parameter

As we mentioned in the Introduction, the exact structure of HVAs is not known, yet it is likely that it consists of 5- and 6-membered rings of hydrogen-bonded water molecules. Therefore, in order to characterize the changes in time of the content of HVAs in the solvation water of AFPs in the analyzed systems, we monitored the changes in the number of 5- and 6-membered rings present in the solvation water. To this aim, we were searching for 5- and 6-membered rings formed by water molecules connected by hydrogen bonds (in this work, we use the “conical” definition of hydrogen bond³⁶). In the calculations, we assumed that a given ring belongs to the analyzed layer, if at least half of the water molecules that build it belong to this layer.

In addition, we used the τ parameter,⁵⁷ which is a measure of the tendency of 5- and 6-membered rings to form more complex, ordered structures. It is defined as the ratio of the number of rings present in the analyzed water layer to the number of water molecules involved in the formation of these rings. When the rings present in the solvation layer are separated, the number of water molecules building them is higher compared to the situation where the rings are interconnected. Thus, the value of the τ parameter becomes higher if the rings create a more connected structure, which gives us information about the “compactness” of the ordered structures formed in solvation water.

As in the case of the order parameter p , we calculated the number of 5- and 6-membered rings and the values of the τ parameter also for the “reference” systems (i.e., fictitious solvation shells). The results are presented in this work as the ratios of either the number of rings present in the solvation water of the protein molecule or the τ parameter in the actual simulation system and in a reference system filled with bulk water (n_{solv}/n_{bulk} and τ_{solv}/τ_{bulk} , respectively).

E. Measurements of the force

As it was mentioned in Sec. II B, in order to measure the force acting on the molecule of AFP III located in the vicinity of ice, one of the atoms of the protein molecule was restrained during simulations at a reference point with the use of a harmonic potential [$k = 10$ kJ/(mol Å²)]. The force was calculated using the method given by Hwang *et al.*,⁵²

$$F_i = \langle r_i - r_{i0} \rangle \frac{k_B T}{\left\{ (r_i - r_{i0})^2 \right\} - \langle r_i - r_{i0} \rangle^2}, i = x, y, z,$$

where \vec{r}_0 stands for the reference coordinates of the selected and restrained protein atoms, \vec{r} is the actual coordinate of the atom, T is the temperature, and k_B is the Boltzmann constant.

III. RESULTS

In our previous study,¹⁸ we have shown that a molecule of hyperactive CfAFP is able to pre-order its solvation water in a way that resembles the structure of ice (in a sense that it is composed of high volume, low energy hydrogen-bonded structures), which allows the molecule of protein to indirectly (via its solvation layer) interact with the crystal of ice. As we discussed in the Introduction (and in Ref. 15), the geometry of these structures escapes precise definition due to their lability, but their building blocks can be 5- and 6-membered rings created by water molecules. Because of that, their content will be measured indirectly. One way would be through calculating the value of an order parameter based on the definition of two-particle entropy. Another approach will be based on the assumption that the more frequent, voluminous, and interconnected these structures become, the higher will be the content of some of their possible building blocks, such as 5- and 6-membered rings (without expecting them to meet any specific requirements regarding the geometry, which means that the rings can be distorted as long as the applied criteria for the existence of hydrogen bonds are met). We have also shown that the ordering of the solvation layer of IBS is not perfect, i.e., the layer is not “ice like” in the literal sense—which is why we referred to it as the “dynamic clathrate.” Here, we would like to show that the conclusions that we have drawn from our previous study for hyperactive CfAFP are more general and can be applied to a moderately active AFP III.

A. Analysis of the solvation water structure

In the first step of our analysis, we used the p order parameter (which is a measure of the structural ordering of water) and the number of 5- and 6-membered rings present in the solvation water (see Sec. II). The calculated values of Δp_{tra} and Δp_{con} determine the position of the point on the “ordering map,” while the ratios n_{solv}/n_{bulk} and τ_{solv}/τ_{bulk} ⁵⁷ reflect the tendency of HVAs’ formation and merging. This analysis was conducted for the fragments of the trajectories in which the distance of the IBS of protein molecule from the original surface of the ice slab was in the range of 1.05–1.15 nm (which was the range of distances that molecules of proteins adopted most commonly in our simulations). We also determined the values of the above-mentioned parameters for the solvation water of ice, and we used them as a convenient reference point; this choice is based on the fact that the process of water solidification proceeds via a gradual remodeling of the liquid structure toward the formation and merging of HVAs.^{28,32} Structural changes, occurring over time in the 0.4 nm-thick solvation layer of both IBS and non-IBS of the AFP III molecule (and its mutant), were analyzed.

In Fig. 2, we presented the changes in the values of Δp_{tra} and Δp_{con} order parameters in time. The positions of the points in the ordering map reflect the change of ordering of water in the analyzed region (for example, in the solvation water of the IBS of AFP III) in relation to the bulk water and are calculated using several independent simulation runs (the exact number depends on the system

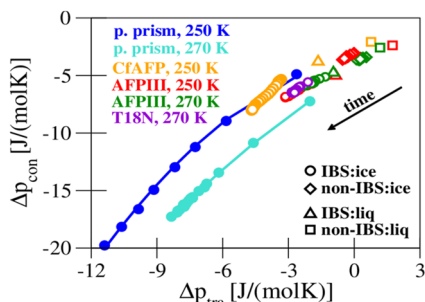


FIG. 2. Ordering map obtained with the use of the values of the order parameters Δp_{tra} and Δp_{con} calculated for the solvation layer of the primary prism plane of ice (dark blue circles), the solvation water of the IBS of the native AFP III molecule facing the primary prism plane of ice at 250 K (red circles) and 270 K (green circles) and the mutated variant (T18N) of AFP III facing the primary prism plane of ice at 270 K (violet circles), the CfAFP molecule facing the primary prism plane of ice at 250 K (orange circles), and the solvation water of the non-IBS of the native AFP III molecule facing the primary prism plane of ice at 250 K (red diamonds) and 270 K (green diamonds). In addition, the results obtained for the solvation water of IBSs of AFP III in liquid water at 250 K (red triangle) and 270 K (green triangle) and CfAFP in liquid water at 250 K (orange triangle), as well as for the solvation water of non-IBSs of AFP III in liquid water at 250 K (red square) and 270 K (green square) and CfAFP in liquid water at 250 K (orange square) are presented. The arrow indicates the direction in which the changes occur in time. In the case of the systems for which changes in time are shown, the simulation times were equal to 12 ns for systems simulated at 250 K and 35 ns for systems simulated at 270 K. For the solvation water of ice simulated at 250 K, only the results up to 5 ns are shown in this figure (the full graph is presented in Fig. S1 of the supplementary material).

considered). As can be seen, when the ice is not present in the vicinity of the AFP III molecule, the ordering of the solvation water of the IBS (red and green up-facing triangles in this figure) is higher than the ordering of the solvation water of the non-IBS (red and green squares). In the case of the non-IBS, we can see that the value of the configurational part of the Δp order parameter is negative but higher than the value obtained for the solvation water of the IBS, while the value of the translational part of this order parameter is positive, showing lower translational ordering compared not only to the solvation water of the IBS but also to bulk water. We have shown previously¹⁸ that the results are similar for the CfAFP molecule (these results are also included in Fig. 2, orange up-facing triangle and square).

When the IBS of AFP III is facing ice (red and green circles), the values of order parameters become increasingly negative over time, reflecting the expected gradual increase in the ordering of solvation water. It can also be seen that the changes are more pronounced at the lower temperature. The results obtained for the T18N mutant of AFP III (violet circles) show the same tendency, suggesting that the mutation in the IBS region, while drastically lowering the biological activity of the protein, has little effect on the overall structure of the solvation water of the IBS. Another observation is that the magnitude of changes that we have observed for the solvation water of the IBS of AFP III and its T18N mutant is smaller compared to the solvation water of the IBS of CfAFP (orange circles). It can be explained by taking into account two main factors. First, the size of the IBS is different in the case of both proteins, which results in the difference in the capacity to facilitate ordering of the solvation water of the IBS.

Second, the distribution of the functionally important groups on the IBS is more regular in the case of CfAFP, allowing water molecules to create a more ordered structure.

In Fig. 2, we have also shown the values of the order parameters obtained for the solvation water of the non-IBS of AFP III when in liquid water (green and red squares) and when facing the ice (green and red diamonds). In both cases, the values are higher than the values obtained for the solvation water of the IBS, indicating that the structure of water is less ordered. In the systems where the non-IBS was facing the ice, we observed that the values of the order parameters change with time in the same direction as it was in the case of the solvation water of the IBS, but the extent of these changes is lower and the values of the order parameters never reach the values corresponding to the solvation water of the IBS.

In order to add even more context to the results presented in the ordering map for the molecules of AFPs, in Fig. 2, we have also presented the results obtained for the solidifying solvation water of the primary prism plane of ice. It can be seen that both the location of the points representing the solvation water of the IBS of AFP III and CfAFP and the direction of the changes with time are similar to the ones obtained for the solvation water of ice. The magnitude of changes with time is higher for the solvation water of ice, which is not surprising when taking into account that the water is freezing. Overall, the results suggest that the solvation water of the IBS of AFP III (and CfAFP¹⁸) is not only more ordered than bulk water or the solvation water of the non-IBS, but also that this ordering is somewhat similar to the ordering observed in the solidifying water.

This conclusion is further supported by the results of the analysis of the number of 5- and 6-membered rings formed by hydrogen-bonded water molecules present in the solvation water of the IBS and the non-IBS of AFP III.

The process of water solidification involves a gradual reorganization of the structure of the liquid, proceeding toward the formation of a hexagonal ice crystal structure; this process is often regarded as the formation of the nuclei of the “ice-like” structure in liquid water. Such an “ice-like” structure is also sought in the solvation water of the IBS of AFP molecules (see Ref. 6 for example). It should be noted, however, that the concept of “ice-like structure” is far from clear, which, as noted by Némethy and Scheraga,²⁶ can lead to numerous misunderstandings; we discussed this more extensively in our previous paper.¹⁵ Generally, the extent of the “ice-likeness” can be defined by specifying the content of those structural elements that can be regarded as “bricks” in the formation of a hexagonal ice cell. This means that such “bricks” must be constructed mainly of 6-membered rings of water molecules connected by hydrogen bonds. We denoted these structures as HVAs (high volume aggregates), emphasizing their most distinctive feature, which is their significant intrinsic volume. It is the higher content of these structures in a liquid that determines its more “ice-like” structure.

Because of that, we decided to monitor the content of the 6-membered rings in solvation water. The content of the 5-membered rings was analyzed as well, although their presence generally counteracts solidification by facilitating transition of the liquid to a glassy state.^{30,31} However, we decided to follow them as well, keeping in mind the observed deformation of the hydrogen bonding network at the protein–ice interface.^{58,59}

In Figs. 3(a) and 3(b), we presented changes in time of the content of the 5- and 6-membered rings in solvation water as an average ratio of the number of rings found in the real solvation layer of the molecule of the protein to the number of rings found in the solvation layer filled with bulk water (see Sec. II), n_{solv}/n_{bulk} . In addition, we show the values of the τ parameter [Fig. 3(c)], which is defined as the number of 5- and 6-membered rings present in the solvation water divided by the number of molecules building these rings. Therefore, the value of the τ parameter is higher when the rings are interconnected and form a larger structure and lower when the rings are separated. In Fig. 3(c), we presented these results as an average τ_{solv}/τ_{bulk} ratio, which gives us information about the compactness of the ring structures formed in the real solvation layer (τ_{solv}) compared to the solvation layer of the same size and shape filled with bulk water (τ_{bulk}).

Let us start with discussing the changes in time of the content of 5- and 6-membered rings in the solvation water of AFPs when their IBSs or non-IBSs are facing the ice surface. From Figs. 3(a) and 3(b), it is clear that the average number of rings in the solvation water of the IBS of AFP III (expressed as the n_{solv}/n_{bulk} ratio) does not change much in time. At 250 K, we can observe a small decrease in the content of 5-membered rings and a small increase in the content of 6-membered rings. In comparison, in the solvation water of the IBS of CfAFP at 250 K, the changes are more pronounced, especially in the case of 6-membered rings. It is also clear from these figures that the observed changes are relatively small in relation to the changes occurring in the solvation water of ice at both 250 and 270 K. An interesting observation is that the average content of the 5-membered rings is almost constant in time for the solvation water of IBSs of AFP III (both the native protein and the T18N mutant) and CfAFP, while for the solvation water of ice, it is gradually decreasing as the process of freezing progresses. These results are consistent with the previous work of Molinero *et al.*,⁵⁸ in which it has been shown that the structure of the solvation water of the IBS of AFP molecules adsorbed onto the surface of ice is not strictly ice-like.

It is also worth noting that the content of 5- and 6-membered rings in the solvation water of the IBS was the highest in the case of T18N mutant—the values are even higher for the AFPs simulated at a lower temperature. This result is consistent with the values of the p order parameters, which were also showing a high degree of ordering in the solvation water of the IBS of the mutant molecule.

The analysis of the changes in time of the τ_{solv}/τ_{bulk} parameter shows how the rings of hydrogen-bonded water molecules in the solvation water of ice gradually form a more interconnected structure as the process of freezing progresses. A similar behavior can be observed for the solvation water of IBSs of AFP III, T18N, and CfAFP, but the value of the τ_{solv}/τ_{bulk} ratio is significantly higher in the case of CfAFP. This result is expected when taking into account the more ordered structure of the IBS of CfAFP and its larger size. The values obtained for the IBS of AFP III facing ice are higher at lower temperatures, which is consistent with the higher content of HVAs in more supercooled water. Overall, observations drawn based on the analysis of the content of ring structures in the solvation water of IBSs support the conclusion of the increasing content of HVAs in the solvation water of IBSs of the studied AFPs over time.

B. Remote interactions between IBS and the surface of ice

We showed previously¹⁵ that in the solvation water of the IBS of the AFP III molecule (which is not in the vicinity of the surface of ice), the content of HVAs is greater than in bulk water. Because the process of freezing of water proceeds through a gradual reorganization of liquid structure toward the formation and merging of HVAs,^{28,32} it can be expected that the structures of interconnected HVAs can act as a kind of a nuclei for solid phase when present in the solvation water of proteins. Therefore, the higher number (compared to bulk water) of these nuclei near the IBS is able to facilitate the transformation of liquid water into ice.

When the IBS is near the surface of the ice crystal, it is expected that HVAs that are already present in its solvation water will be additionally stabilized by interacting with the solvation water of the ice crystal. However, this will only be the case if the distance between the ice and the protein matches the size of the HVAs—otherwise, the HVAs will be destroyed by their compression or stretching, as we discussed previously¹⁸ when analyzing a hyperactive CfAFP molecule in the vicinity of ice.

In order to test whether this argumentation can also be applied to the AFP III molecule, we conducted molecular dynamics simulations of AFP III and T18N mutant facing the primary prism plane of ice with their IBSs and of AFP III facing the primary prism plane of ice with its non-IBS, at 270 K. The distance between the molecules of the proteins and the ice was equal to around 1 nm (see Sec. II).

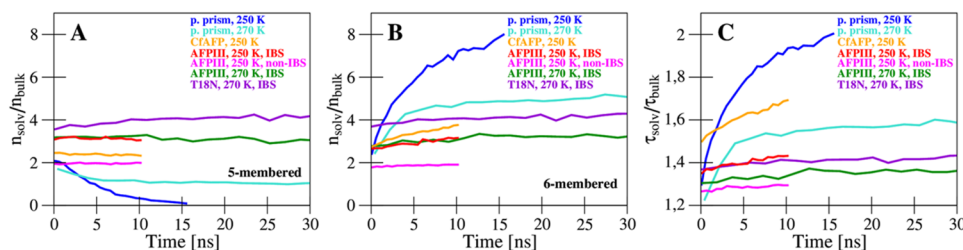


FIG. 3. Changes in time of the average content of 5- and 6-membered rings in the solvation water of AFPs and ice expressed as a n_{solv}/n_{bulk} ratio [(a) and (b), respectively] and changes in time of the average values of the τ parameter expressed as a τ_{solv}/τ_{bulk} ratio (c). The estimated standard deviations of the means are in the range of 0.05–0.20 in the case of panels (a) and (b) and in the range of 0.01–0.03 in the case of panel (c).

It is worth noting here that the IBS of the AFP III molecule is relatively flat, and when it is parallel to the ice surface, its distance from the ice can be easily defined. However, when the (flat) IBS forms a certain angle with the plane of the ice crystal, it becomes difficult to propose a proper definition of this distance. It is also impossible to unambiguously define the distance from the non-IBS to the surface of ice, since the non-IBS has a very irregular shape. Therefore, when analyzing the changes in the position of the *protein* molecules with respect to the surface of ice, we consider two parameters: the distance of the AFP molecule's center of mass from this surface and the angle of inclination of the plane approximating the IBS to the surface of ice. To complete the description, let us mention that the center of mass of the AFP III molecule is around 1.0 nm away from the plane approximating the IBS.

The results obtained for distance measurements are presented in Fig. 4. For comparison, we included the corresponding figures illustrating the behavior of the *CfAFP* protein under similar conditions (at 265 K, results obtained previously¹⁶) in the supplementary material. Moreover, for the systems in which the AFP III and T18N molecules were facing the surface of ice with their IBSs, we also analyzed the changes with time of the inclination angle of the plane approximating the IBS of the protein molecule with respect to the ice plane. We have shown these results in Fig. S2 of the supplementary material.

The main conclusion that can be drawn from Fig. 4 is that AFP III and T18N molecules that face the primary prism plane of ice with their IBSs tend to maintain a constant distance from the original ice slab in time. We can see that the location of the maxima of the distributions of the distances is not changing much in time; however, there are some protein molecules (more in the case of the native variant) for which the distance from the ice surface changes significantly in the course of the simulation. In addition, the analysis of the change in the inclination angles of the IBSs of the native and mutant variants of AFP III with the protein–ice distance (Fig. S2 of the supplementary material) shows that the protein molecules that stay in the range of distance close to the maxima of the distributions from Figs. 4(a) and 4(b) tend to maintain a roughly parallel orientation of their IBSs relative to the surface of ice. The behavior of the systems in which the AFP III molecule was facing the ice with its non-IBS is different—as it can be seen in Fig. 4(c), the changes with time of the distance between protein molecules and ice seem to be more chaotic, resulting from diffusion movements. This behavior is very similar to that observed by us previously¹⁶ for the hyperactive *CfAFP* (see also Fig. S3 of the supplementary material) protein and to the results reported by Kumari *et al.*³⁵ The authors showed that

the AFP III molecule (wild type or its mutant) moves away from the surface of growing ice (primary prism plane) in about 20% of the cases when it is facing the ice with its IBS. Meanwhile, a molecule of ubiquitin, which lacks the antifreeze activity, moved away from the ice in about 85% of the cases.

The results presented in Fig. 4 and Fig. S3 show that the main difference between the behavior of the systems containing the *CfAFP* and AFP III molecules that were facing the surface of ice with their IBSs is the frequency with which the protein molecules tend to stay in the certain (optimal) range of distances from the surface of ice. In the case of *CfAFP*, we observed that this behavior is more common (~15% to 20% of 240 molecules simulated at 265 K left the optimal range of distances; Fig. S3 of the supplementary material), whereas in systems containing AFP III, molecules tended to stay within the optimal distance from the surface of ice about 50% of the time [Fig. 4(a)]. The distinctly higher (compared to the results obtained for the *CfAFP* protein) tendency of the AFP III molecules to move away from the primary prism plane of ice can be explained by comparing the size of the ice binding sites of both of these proteins. The ice binding site of AFP III is clearly smaller, and thus, the strength of the interaction of this molecule with ice is lower. The dependence of the strength of the interaction of AFPs with ice on the size of the IBS has previously been shown by other authors.^{60–63} It is worth noting here, however, that the conditions under which the observations were carried out for these two proteins were slightly different. Namely, changes in the distance of the *CfAFP* molecules from the crystal surface were studied in systems containing a cuboidal ice crystal and simulated at a lower temperature (at 265 K, results obtained before¹⁶). Therefore, the comparison of the behavior of these two proteins is only approximate.

Another interesting observation is that the molecules of the T18N mutant [Fig. 4(b)] were more likely to stay closer to the surface of ice compared to the native AFP III molecules. This is another instance where we can see that the early interactions with the surface of ice seem to be more favorable in the case of the T18N molecule, even though its biological activity is equal to only 10% of the activity of the native variant.⁴⁴ Therefore, the results suggest that the reason for the lowered activity of the mutant is not the inability of the protein molecule to recognize and interact with ice at the early stages of the process of adsorption of the protein onto the ice. This conclusion is consistent with the results of a recent experimental study,³⁷ which showed that the T18N mutant of the AFP III molecule was still able to adsorb onto the surface of ice, but the adsorption was reversible, contrarily to the irreversible adsorption observed in the case of the native AFP III.

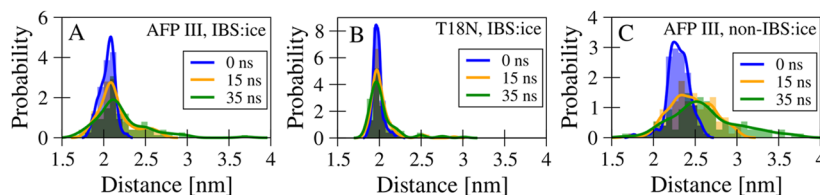


FIG. 4. Changes with time of the distance between the center of mass of an AFP III molecule and ice presented as the distributions of the distances at 0, 15, and 35 ns. In these figures, the type of the protein molecule (AFP III or T18N) and the part of the protein molecules facing the primary prism plane of ice (IBS or non-IBS) are specified. The distance of the center of mass of the *protein* molecule from its IBS is around 1.0 nm.

In Fig. 4 and Fig. S2, we observed a tendency of the AFP III molecule (both native and mutated variants) to maintain a constant distance and orientation with respect to the surface of the ice crystal (when facing the ice with its IBS). In discussion, we used a term “optimal” when referring to the distances between the protein molecules and ice that were most commonly adopted in the analyzed systems. As we mentioned before, the HVAs present in the solvation water of the IBS can interact with the solvation water of the ice crystal. Since HVAs have a certain volume, it can be expected that some ranges of distances between the HVAs’ surfaces of protein and ice are preferred in order to maintain HVAs’ integrity—we refer to these distances as being “optimal.”

We tested whether this assumption is true by measuring the force acting on the AFP III molecule located in the proximity of the ice surface at several different distances—the results are shown in Fig. 5. The systems were prepared following the same procedure as

in the case of CfAFP¹⁸—they consisted of a block of ice and AFP III molecules located in the vicinity of its sides [see Fig. 1(b)] and were simulated at 250 K.

In Fig. 5, we presented the average change of the force acting on a protein molecule (native variant) with the distance between the IBS or non-IBS of the protein and the surface of ice. The main conclusion from this figure is the clear difference between the course of the curves when the AFP III molecule was facing ice with its IBS and non-IBS. In the case of protein molecules facing the ice with the IBS, the average force acting on the molecules was almost constant regardless of the distance from the ice. Some changes are visible in the course of the curves—local minima and maxima—but they are not as prominent as it was in the case of the results for CfAFP. For molecules facing ice with their non-IBS, a clear increase in the average force with the decrease in the protein–ice distance can be seen. This force is responsible for repelling protein molecules away from the surface of ice, preventing their adsorption.

While the analysis of the changes in the average values of force acting on AFP III molecules with their distance from ice can provide a general picture of the process of interaction of AFP III with the surface of ice, it is interesting to examine it in more detail. In Fig. 5, we presented the distribution of the values of force acting on molecules of AFP III (facing the ice with either the IBS or the non-IBS) in different ranges of distances. As it can be seen, in the case of molecules of protein facing the ice with the non-IBS (orange lines), the maxima of the distributions tend to have a positive value, indicating that the force tries to repel the molecules of protein away from the surface of ice. In the case of AFP III molecules facing ice with the IBS (blue lines), distributions tend to be broader, with more instances of the force being strongly positive or negative. Depending on the range of protein–ice distances, the distributions are more or less shifted toward the positive values of force, consistent with the previous observation that AFP III molecules facing the ice with the IBS tend to move away from the surface of ice in some cases.³⁵ For comparison, in Fig. 5, we also added the results obtained for the CfAFP molecule facing the ice with its IBS. As can be seen, the behavior is similar to that of AFP III, but the effects are more distinct in the case of CfAFP molecules. From this figure, it can be concluded that the molecules of both AFPs facing the ice with their IBSs show the ability of positioning themselves in an optimal position in relation to the ice, while the molecules facing the ice with the non-IBS are either repelled from the ice if the distance becomes too small or they change the positions due to diffusion movements.

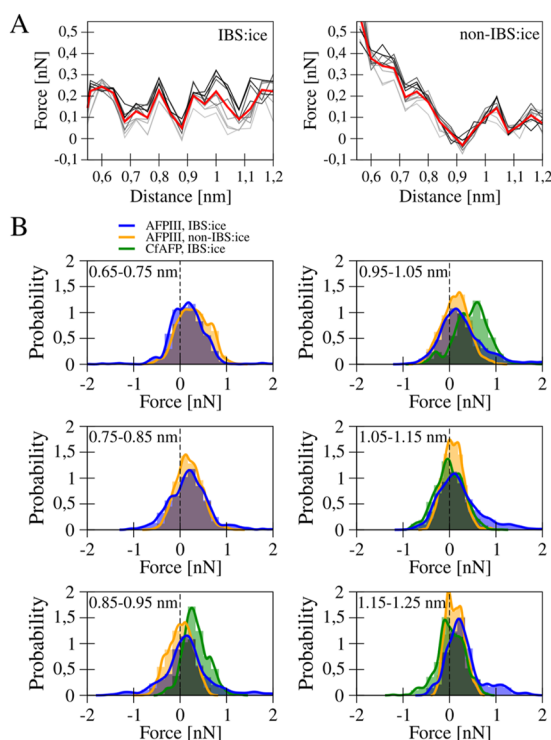


FIG. 5. (a) Average values of a force acting on the AFP III molecule facing ice with its IBS or non-IBS and located at different distances from the surface of the primary prism plane of ice. The gray lines represent the changes in the average values of the force with time (the lightest line—0 ns, the darkest—35 ns), while the red lines show the average values of the force acting on the protein molecules for the entirety of the simulations. (b) Distributions of the values of the force acting on AFP III molecules that face the ice with their IBS (blue lines) or non-IBS (orange lines). For comparison, the results obtained previously¹⁸ for CfAFP molecules facing the ice with their IBS are also shown (green lines). The distance of the AFP III molecule from ice was measured between the center of mass of the five atoms located within the IBS or CB atom of PRO57 located within the non-IBS and the plane passing through the oxygen atoms of water molecules building the original surface of the ice crystal. To allow comparison with the results shown in Fig. 4, note that the distance from the center of mass of the AFP III molecule to its IBS is around 1.0 nm.

C. The anchoring of HVAs to the protein surface

In the Introduction, we defined HVAs as structurally ordered objects that appear in increasing amount during the solidification process. Contrary to locally favored structures (LFSs) defined by Tanaka,²⁵ we do not consider HVAs as rare; the frequency of their formation in solvation water depends on the temperature and the type of the solvated surface.¹⁵ Moreover, HVAs are not spatially restricted, that is, they do not have to meet the “short-range order” criterion formulated by Tanaka.²⁵ The existence of such relatively large HVAs was used by us previously¹⁸ to explain the characteristic periodic course (observed at relatively long distances, reaching 1 nm) of the AFP–ice interaction energy curve as a function of their

distance, as well as a similar interaction energy curve of two *RiAFP* molecules obtained at 300 K by Mochizuki and Matsumoto.⁶⁴

Assuming that, on the IBSs of AFPs, there are certain “hot spots” where molecules of solvation water bind with the surface of the protein molecule, it should be expected that the anchoring of HVAs will occur at these points. In addition, the anchoring may also be responsible for an additional stabilization of the structure of HVAs. Thus, the set of water molecules that are located in the vicinity of the aforementioned “hot spots” on the IBS of an AFP molecule becomes a more labile equivalent of the anchored clathrate concept described by Garnham *et al.*¹⁰ Based on our results, we argue that the anchoring of HVAs simultaneously on the IBS of an AFP molecule and on the surface of the ice crystal is a necessary preliminary step of the process of adsorption of AFPs on the surface of the ice crystal.¹⁸

In order to find the “hot spots” on the IBS of the AFP III molecule, we determined the most probable locations of water molecules in the vicinity of the IBS. We divided the space around the IBS into cubic cells with an edge length of 0.02 nm, and we chose the cells in which the probability of finding either an oxygen or a hydrogen atom exceeded the value obtained for bulk water at least ten times. The results of this analysis are presented in Fig. S4 of the supplementary material. This figure clearly shows the clustering of the cells with the high probability of finding water molecules in certain small spatial areas.

In the next step, we determined the average positions of the oxygen atoms in these areas in order to compare them to the positions of the oxygen atoms in the crystal lattice of ice. First, the AFP III molecule was superimposed on the crystal lattice of ice in a way that the IBS of the protein was parallel to the primary prism plane of ice. Then, by changing the location and orientation of the molecule of AFP III in relation to the lattice of ice, we searched for the position in which the average distance between the “hot spots” on the IBS and the oxygen atoms in the ice lattice was the smallest. As a result, we found that the most probable positions of the oxygen atoms of water molecules in the solvation water of the IBS match the crystal lattice of ice relatively well, which is illustrated in Fig. 6. The average value of the distance between the “hot spots” and the oxygen atoms in the ice lattice in this configuration is equal to 0.786 Å. A very similar value (0.77 Å) was reported previously by Khan *et al.*¹³ for moderately active *TisAFP7* in relation to the basal plane of ice. Although

the match is not perfect, it should be considered sufficient since—as shown by Hudait *et al.*⁵⁸—the nodes of the crystal lattice of ice that are directly bound to the IBS of an AFP molecule deviate from their “ideal” positions.

D. The model of interaction of an AFP molecule with the surface of ice

The presented data allow us to describe a more general model of the initial stages of the interaction of AFPs with the ice. In the first step of the argumentation, we postulate that the equilibrium between the HVAs and disordered phase shifts in the solvation water of proteins (compared to bulk water). This is a consequence of the interactions between the liquid water and the surface of the solute molecule (e.g., protein). Depending on the geometry and chemical nature of the hydrated surface, HVAs will, due to interactions with this surface, undergo either destruction or additional stabilization. In the vicinity of the surface of an “ordinary” protein molecule, HVAs are destroyed.³³ However, we have shown that in the vicinity of the IBS of *CfAFP*¹⁸ and AFP III molecules, the balance between the two structural forms of water is shifted in the opposite direction, enhancing the tendency to form HVAs. We can assume that the same should be true in the vicinity of IBSs of other AFPs, i.e., the balance is shifted toward enhancing the tendency to form HVAs. Since the process of water freezing proceeds through a gradual remodeling of the structure of liquid in the direction of HVAs’ formation and merging,^{28,32} it can be said that in a way the HVAs anchored to the IBS create a form of embryo for the solid phase.

Now, suppose that the IBS of the AFP molecule under consideration is located close to the ice surface. In the second step of our argumentation, we assume that HVAs already anchored onto the IBS can be additionally stabilized by interacting with the solvation water of the adjacent ice surface. This process facilitates the transformation of solvation water of the IBS into a solid phase, while the anchoring of HVAs to both IBS and ice is responsible for the final (irreversible) adsorption of the AFP molecule to the ice. However, this will only be possible if the distance between the IBS and the ice surface matches the size of HVAs; otherwise, they will be crushed or torn. Such destruction naturally involves a certain energy cost;

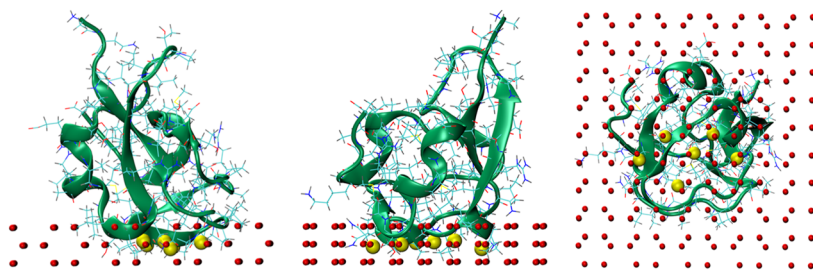


FIG. 6. Matching of the most probable positions of solvation water molecules of the IBS of the AFP III molecule (represented by the positions of their oxygen atoms, yellow spheres) to the positions of the oxygen atoms in the crystal lattice of the primary prism plane of ice (red spheres). The centers of the yellow spheres are located in the centers of the areas with the highest probabilities of finding the oxygen atoms of the solvation water molecules (see Fig. S4 of the supplementary material), while the diameter of the spheres roughly reflects the size of these areas. The average distance between the centers of mass of the yellow spheres from the closest positions of the oxygen atoms in the ice lattice is equal to 0.786 Å. The picture was generated in VMD.⁵¹

so, consequently, a characteristic cyclic (as a function of a distance) course of the potential energy curve of the interaction of the IBS with ice is expected. In our studies, we confirmed that such a pattern is observed for both the hyperactive protein CfAFP¹⁸ and (to a lesser extent) AFP III. Additional confirmation of the validity of the presented argument is given by the observation of an analogous “cyclic” profile of the potential energy curve of the interaction (as a function of a distance) between the IBSs of two RiAFP molecules in water,⁶⁴ although, in this case, HVAs are anchored simultaneously to the IBSs of neighboring RiAFP molecules.

The presented reasoning, describing the process of adsorption of an AFP molecule onto the surface of ice, assigns the key role in this process to the natural tendency of liquid water to form HVAs that have the ability to anchor onto the solvated surface (protein molecule or ice crystal). As a result of this anchoring, already at distances exceeding 1 nm, we observed the effect of positioning of the AFPs at a certain distances relative to the surface of ice. Simultaneously, the structure of solvation water of the IBS that interacts with ice becomes more ordered and “ice-like” with time. This process is relatively slow (compared to the time scale characterizing the dynamics of solvation water) and involves a gradual increase in HVAs’ content and their merging into larger aggregates.^{28,32} Thus, a crystalline network of ice is progressively building up in the solvation water, which already *in statu nascendi* remains bound to both the IBS and ice surfaces.

However, as we mentioned in the Introduction, the initial recognition and interaction of AFPs with the surface of ice do not necessarily guarantee their successful binding. While we do not observe any dramatic differences between the properties of solvation water of the IBS of wild-type AFPs and mutants of lower activity, their ice-binding propensities can differ very strongly. Mutants of AFPs that have very little to no activity can interact with the ice too,³⁷ but in the case of fully active AFPs, this process occurs much more frequently (due to the more favorable interactions with the ice) which allows for the inhibition of the ice growth. We also cannot say that the lack of the long-range ordering of water prohibits the incorporation into the ice in every circumstance. For example, it has been observed that, in some cases, a molecule that does not display any antifreeze activity may be frozen into the ice.^{35,36}

IV. CONCLUSIONS

The AFP molecule binds onto the ice surface via a system of hydrogen bonds. However, in order to create such a system of bonds, it is necessary to precisely align both interacting surfaces: the ice and the IBS of the AFP. In our previous work^{16–18} and currently, we showed that this alignment is, by no means, achieved by chaotic diffusion movements—on the contrary, there is a clearly directional interaction between the IBS and the ice surface, whose role is to position the AFP molecule in such a way that will eventually allow it to bind onto the ice surface. The range of this interaction exceeds 1 nm, and the mediating factor is the layer of solvation water.

The existence of such an interaction has not been described by other authors so far, although its existence has previously been considered.^{6,59} In our opinion, its presence is a necessary (though not sufficient) condition for the adsorption process to be effective, while the use of contemporary models of water structure has allowed us to understand its mechanism.

In our study, we showed that the moderately active AFP III molecule interacts with the ice surface according to the mechanism that is analogous to the one we proposed before for the hyperactive CfAFP molecule.¹⁸ We described the process of “remote” positioning of the protein molecule in relation to the ice surface and the cyclic changes of the force acting on the protein molecule with its distance from the ice surface when it was facing the ice with its IBS.

In addition, the results presented in this work for AFP III are in full agreement with the ones obtained by us previously for hyperactive CfAFP, which indicates that both molecules interact with the ice according to the same mechanism. Thus, the mechanism remains unchanged despite significant differences in the molecular structure of the ice binding sites of these molecules (i.e., both the size of the ice binding sites and the way atoms are arranged on their surfaces). This confirms, strongly emphasized in this paper, the key role played by the solvation water (through the presence of HVAs) in the adsorption process. In our opinion, this allows us to speculate that also other types of AFPs probably interact with the ice surface according to an analogous mechanism.

SUPPLEMENTARY MATERIAL

The supplementary material contains additional figures presenting the results of the calculations of the order parameter, the inclination angles of the IBS of AFP III in relation to the surface of ice and changes in the distance of CfAFP molecule from the ice surface in time, and the most probable positions of the oxygen and hydrogen atoms of water molecules of solvation water of the IBS of the AFP III molecule.

ACKNOWLEDGMENTS

We gratefully acknowledge Poland’s high-performance Infrastructure PLGrid (HPC Centers: ACK Cyfronet AGH, PCSS, CI TASK, WCSS) for providing computer facilities and support within computational Grant No. PLG/2023/016528. Computations were carried out using the computers of Centre of Informatics Tricity Academic Supercomputer and Network.

AUTHOR DECLARATIONS

Conflict of Interest

The authors have no conflicts to disclose.

Author Contributions

Joanna Grabowska: Conceptualization (equal); Data curation (equal); Formal analysis (equal); Investigation (equal); Methodology (equal); Supervision (equal); Writing – original draft (equal); Writing – review & editing (equal). **Anna Kuffel:** Conceptualization (equal); Data curation (equal); Formal analysis (equal); Investigation (equal); Methodology (equal); Supervision (equal); Writing – original draft (equal); Writing – review & editing (equal). **Jan Zielkiewicz:** Conceptualization (equal); Data curation (equal); Formal analysis (equal); Investigation (equal); Methodology (equal); Supervision (equal); Writing – original draft (equal); Writing – review & editing (equal).

DATA AVAILABILITY

The data that support the findings of this study are available from the corresponding author upon reasonable request.

REFERENCES

- ¹Y. Celik, L. A. Graham, Y.-F. Mok, M. Bar, P. L. Davies, and I. Braslavsky, "Superheating of ice crystals in antifreeze protein solutions," *Proc. Natl. Acad. Sci. U. S. A.* **107**, 5423–5428 (2010).
- ²Y. Celik, R. Drori, N. Pertaya-Braun, A. Altan, T. Barton, M. Bar-Dolev, A. Groisman, P. L. Davies, and I. Braslavsky, "Microfluidic experiments reveal that antifreeze proteins bound to ice crystals suffice to prevent their growth," *Proc. Natl. Acad. Sci. U. S. A.* **110**, 1309–1314 (2013).
- ³R. Drori, P. L. Davies, and I. Braslavsky, "When are antifreeze proteins in solution essential for ice growth inhibition?," *Langmuir* **31**, 5805–5811 (2015).
- ⁴A. L. Devries and Y. Lin, "Structure of a peptide antifreeze and mechanism of adsorption to ice," *Biochim. Biophys. Acta, Protein Struct.* **495**, 388–392 (1977).
- ⁵N. Smolin and V. Daggett, "Formation of ice-like water structure on the surface of an antifreeze protein," *J. Phys. Chem. B* **112**, 6193–6202 (2008).
- ⁶D. R. Nutt and J. C. Smith, "Dual function of the hydration layer around an antifreeze protein revealed by atomistic molecular dynamics simulations," *J. Am. Chem. Soc.* **130**, 13066–13073 (2008).
- ⁷Y. Xu, R. Gnanasekaran, and D. M. Leitner, "Analysis of water and hydrogen bond dynamics at the surface of an antifreeze protein," *J. At., Mol., Opt. Phys.* **2012**, 1–6.
- ⁸K. Meister, S. Ebbinghaus, Y. Xu, J. G. Duman, A. DeVries, M. Gruebele, D. M. Leitner, and M. Havenith, "Long-range protein-water dynamics in hyperactive insect antifreeze proteins," *Proc. Natl. Acad. Sci. U. S. A.* **110**, 1617–1622 (2013).
- ⁹K. Meister, S. Strazdaite, A. L. DeVries, S. Lotze, L. L. C. Olijve, I. K. Voets, and H. J. Bakker, "Observation of ice-like water layers at an aqueous protein surface," *Proc. Natl. Acad. Sci. U. S. A.* **111**, 17732–17736 (2014).
- ¹⁰C. P. Garnham, R. L. Campbell, and P. L. Davies, "Anchored clathrate waters bind antifreeze proteins to ice," *Proc. Natl. Acad. Sci. U. S. A.* **108**, 7363–7367 (2011).
- ¹¹K. A. Sharp, "A peek at ice binding by antifreeze proteins," *Proc. Natl. Acad. Sci. U. S. A.* **108**, 7281–7282 (2011).
- ¹²A. J. Middleton, C. B. Marshall, F. Faucher, M. Bar-Dolev, I. Braslavsky, R. L. Campbell, V. K. Walker, and P. L. Davies, "Antifreeze protein from freeze-tolerant grass has a beta-roll fold with an irregularly structured ice-binding site," *J. Mol. Biol.* **416**, 713–724 (2012).
- ¹³N. M.-M. U. Khan, T. Arai, S. Tsuda, and H. Kondo, "Characterization of microbial antifreeze protein with intermediate activity suggests that a bound-water network is essential for hyperactivity," *Sci. Rep.* **11**, 5971 (2021).
- ¹⁴A. Hudait, D. R. Moberg, Y. Qiu, N. Odendahl, F. Paesani, and V. Molinero, "Preordering of water is not needed for ice recognition by hyperactive antifreeze proteins," *Proc. Natl. Acad. Sci. U. S. A.* **115**, 8266–8271 (2018).
- ¹⁵J. Zielkiewicz, "Mechanism of antifreeze protein functioning and the "anchored clathrate water" concept," *J. Chem. Phys.* **159**, 085101 (2023).
- ¹⁶J. Grabowska, A. Kuffel, and J. Zielkiewicz, "Molecular dynamics study on the role of solvation water in the adsorption of hyperactive AFP to the ice surface," *Phys. Chem. Chem. Phys.* **20**, 25365–25376 (2018).
- ¹⁷J. Grabowska, A. Kuffel, and J. Zielkiewicz, "Role of the solvation water in remote interactions of hyperactive antifreeze proteins with the surface of ice," *J. Phys. Chem. B* **123**, 8010–8018 (2019).
- ¹⁸J. Grabowska, A. Kuffel, and J. Zielkiewicz, "Interfacial water controls the process of adsorption of hyperactive antifreeze proteins onto the ice surface," *J. Mol. Liq.* **306**, 112909 (2020).
- ¹⁹O. A. Karim and A. D. J. Haymet, "The ice/water interface: A molecular dynamics simulation study," *J. Chem. Phys.* **89**, 6889–6896 (1988).
- ²⁰D. Beaglehole and P. Wilson, "Thickness and anisotropy of the ice-water interface," *J. Phys. Chem.* **97**, 11053–11055 (1993).
- ²¹M. M. Conde, C. Vega, and A. Patrykiewicz, "The thickness of a liquid layer on the free surface of ice as obtained from computer simulation," *J. Chem. Phys.* **129**, 014702 (2008).
- ²²S. Cui, W. Zhang, X. Shao, and W. Cai, "Do antifreeze proteins generally possess the potential to promote ice growth?," *Phys. Chem. Chem. Phys.* **24**, 7901–7908 (2022).
- ²³A. Kuffel, D. Czapiewski, and J. Zielkiewicz, "Unusual structural properties of water within the hydration shell of hyperactive antifreeze protein," *J. Chem. Phys.* **141**, 055103 (2014).
- ²⁴S. Del Galdo, P. Marracino, M. D'Abramo, and A. Amadei, "In silico characterization of protein partial molecular volumes and hydration shells," *Phys. Chem. Chem. Phys.* **17**, 31270–31277 (2015).
- ²⁵H. Tanaka, "Simple physical model of liquid water," *J. Chem. Phys.* **112**, 799–809 (2000).
- ²⁶G. Némethy and H. A. Scheraga, "Structure of water and hydrophobic bonding in proteins. I. A model for the thermodynamic properties of liquid water," *J. Chem. Phys.* **36**, 3382–3400 (1962).
- ²⁷H. Tanaka, "Simple physical explanation of the unusual thermodynamic behavior of liquid water," *Phys. Rev. Lett.* **80**, 5750–5753 (1998).
- ²⁸F. H. Stillinger, "Water revisited," *Science* **209**, 451–457 (1980).
- ²⁹H. Tanaka, "General view of a liquid-liquid phase transition," *Phys. Rev. E* **62**, 6968–6976 (2000).
- ³⁰H. Tanaka, "Thermodynamic anomaly and polyamorphism of water," *Europhys. Lett.* **50**, 340–346 (2000).
- ³¹H. Tanaka, "Two-order-parameter description of liquids. I. A general model of glass transition covering its strong to fragile limit," *J. Chem. Phys.* **111**, 3163–3174 (1999).
- ³²J. Russo and H. Tanaka, "Understanding water's anomalies with locally favoured structures," *Nat. Commun.* **5**, 3556 (2014).
- ³³A. Kuffel and J. Zielkiewicz, "Why the solvation water around proteins is more dense than bulk water," *J. Phys. Chem. B* **116**, 12113–12124 (2012).
- ³⁴P. W. Wilson, K. E. Osterday, A. F. Heneghan, and A. D. J. Haymet, "Type I antifreeze proteins enhance ice nucleation above certain concentrations," *J. Biol. Chem.* **285**, 34741–34745 (2010).
- ³⁵S. Kumari, A. V. Muthachikavil, J. K. Tiwari, and S. N. Punnathanam, "Computational study of differences between antifreeze activity of type-III antifreeze protein from ocean pout and its mutant," *Langmuir* **36**, 2439–2448 (2020).
- ³⁶P. Pal, R. Aich, S. Chakraborty, and B. Jana, "Molecular factors of ice growth inhibition for hyperactive and globular antifreeze proteins: Insights from molecular dynamics simulation," *Langmuir* **38**, 15132–15144 (2022).
- ³⁷R. P. Tas, M. M. R. M. Hendrix, and I. K. Voets, "Nanoscopy of single antifreeze proteins reveals that reversible ice binding is sufficient for ice recrystallization inhibition but not thermal hysteresis," *Proc. Natl. Acad. Sci. U. S. A.* **120**, e2212456120 (2023).
- ³⁸D. A. Case, R. . Betz, D. S. Cerutti, T. E. Cheatham, T. A. Darden, R. E. Duke, T. Giese, H. Gohlke, A. W. Goetz, N. Homeyer, S. Izadi, P. Janowski, J. Kaus, A. Kovalenko, T. S. Lee, S. LeGrand, P. Li, C. Lin, T. Luchko, R. Luo, B. Madej, D. Mermelstein, K. M. Merz, G. Monard, H. Nguyen, H. T. Nguyen, I. Omelyan, A. Onufriev, D. R. Roe, A. Roitberg, C. Sagui, C. L. Simmerling, W. M. Botello-Smith, J. Swails, R. C. Walker, J. Wang, R. M. Wolf, X. Wu, L. Xiao, and P. A. Kollman, *Amber 16*, University of California, San Francisco, 2016.
- ³⁹H. J. C. Berendsen, J. P. M. Postma, W. F. van Gunsteren, A. DiNola, and J. R. Haak, "Molecular dynamics with coupling to an external bath," *J. Chem. Phys.* **81**, 3684–3690 (1984).
- ⁴⁰J. L. F. F. Abascal, E. Sanz, R. García Fernández, C. Vega, R. G. Fernández, and C. Vega, "A potential model for the study of ices and amorphous water: TIP4P/Ice," *J. Chem. Phys.* **122**, 234511 (2005).
- ⁴¹R. G. Fernández, J. L. F. Abascal, and C. Vega, "The melting point of ice Ih for common water models calculated from direct," *J. Chem. Phys.* **124**, 144506 (2006).
- ⁴²Z. Jia, C. I. DeLuca, H. Chao, and P. L. Davies, "Structural basis for the binding of a globular antifreeze protein to ice," *Nature* **384**, 285–288 (1996).
- ⁴³C. L. Hew, N. C. Wang, S. Joshi, G. L. Fletcher, G. K. Scott, P. H. Hayes, B. Buettner, and P. L. Davies, "Multiple genes provide the basis for antifreeze protein diversity and dosage in the ocean pout, *Macrozoarces americanus*," *J. Biol. Chem.* **263**, 12049–12055 (1988).
- ⁴⁴S. P. Graether, C. I. DeLuca, J. Baardsnes, G. A. Hill, P. L. Davies, and Z. Jia, "Quantitative and qualitative analysis of type III antifreeze protein structure and function," *J. Biol. Chem.* **274**, 11842–11847 (1999).

- ⁴⁵M. D. Ekpo, J. Xie, Y. Hu, X. Liu, F. Liu, J. Xiang, R. Zhao, B. Wang, and S. Tan, "Antifreeze proteins: Novel applications and navigation towards their clinical application in cryobanking," *Int. J. Mol. Sci.* **23**, 2639 (2022).
- ⁴⁶M. D. Smallwood-Worrall, L. Byass, L. Elias, D. Ashford, C. J. Doucet, C. Holt, J. Telford, P. Lillford, and D. J. Bowles, "Isolation and characterization of a novel antifreeze protein from carrot (*Daucus carota*)," *Biochem. J.* **340**, 385–391 (1999).
- ⁴⁷L. A. Graham, Y. C. Liou, V. K. Walker, and P. L. Davies, "Hyperactive antifreeze protein from beetles," *Nature* **388**, 727–728 (1997).
- ⁴⁸M. J. Kuiper, C. J. Morton, S. E. Abraham, and A. Gray-Weale, "The biological function of an insect antifreeze protein simulated by molecular dynamics," *Elife* **4**, e05142 (2015).
- ⁴⁹J. Baardsnes and P. L. Davies, "Contribution of hydrophobic residues to ice binding by fish type III antifreeze protein," *Biochim. Biophys. Acta, Protein Struct.* **1601**, 49–54 (2002).
- ⁵⁰C. P. Garnham, A. Natarajan, A. J. Middleton, M. J. Kuiper, I. Braslavsky, and P. L. Davies, "Compound ice-binding site of an antifreeze protein revealed by mutagenesis and fluorescent tagging," *Biochemistry* **49**, 9063–9071 (2010).
- ⁵¹W. Humphrey, A. Dalke, and K. Schulten, "VMD: Visual molecular dynamics," *J. Mol. Graphics* **14**, 33–38 (1996).
- ⁵²W. Hwang, M. J. Lang, and M. Karplus, "Force generation in kinesin hinges on cover-neck bundle formation," *Structure* **16**, 62–71 (2008).
- ⁵³J. Zielkiewicz, "Two-particle entropy and structural ordering in liquid water," *J. Phys. Chem. B* **112**, 7810–7815 (2008).
- ⁵⁴H. S. Green, *The Molecular Theory of Fluids* (North-Holland, Amsterdam, 1952), Chap. III.
- ⁵⁵R. Esposito, F. Saija, A. Marco Saitta, and P. V. Giaquinta, "Entropy-based measure of structural order in water," *Phys. Rev. E* **73**, 040502 (2006).
- ⁵⁶P. Wernet, D. Nordlund, U. Bergmann, M. Cavalleri, M. Odelius, H. Ogasawara, L. A. Näslund, T. K. Hirsch, L. Ojamäe, P. Glatzel, L. G. M. Pettersson, and A. Nilsson, "The structure of the first coordination shell in liquid water," *Science* **304**, 995–999 (2004).
- ⁵⁷J. Grabowska, A. Kuffel, and J. Zielkiewicz, "Revealing the Frank–Evans "iceberg" structures within the solvation layer around hydrophobic solutes," *J. Phys. Chem. B* **125**, 1611–1617 (2021).
- ⁵⁸A. Hudait, N. Odendahl, Y. Qiu, F. Paesani, and V. Molinero, "Ice-nucleating and antifreeze proteins recognize ice through a diversity of anchored clathrate and ice-like motifs," *J. Am. Chem. Soc.* **140**, 4905–4912 (2018).
- ⁵⁹S. Mahatabuddin, D. Fukami, T. Arai, Y. Nishimiya, R. Shimizu, C. Shibasaki, H. Kondo, M. Adachi, and S. Tsuda, "Polypentagonal ice-like water networks emerge solely in an activity-improved variant of ice-binding protein," *Proc. Natl. Acad. Sci. U. S. A.* **115**, 5456–5461 (2018).
- ⁶⁰K. Liu, Z. Jia, G. Chen, C. Tung, and R. Liu, "Systematic size study of an insect antifreeze protein and its interaction with ice," *Biophys. J.* **88**, 953–958 (2005).
- ⁶¹D. J. Kozuch, F. H. Stillinger, and P. G. Debenedetti, "Combined molecular dynamics and neural network method for predicting protein antifreeze activity," *Proc. Natl. Acad. Sci. U. S. A.* **115**, 13252–13257 (2018).
- ⁶²C. B. Marshall, M. E. Daley, B. D. Sykes, and P. L. Davies, "Enhancing the activity of a β -helical antifreeze protein by the engineered addition of coils," *Biochemistry* **43**, 11637–11646 (2004).
- ⁶³C. L. Scholl and P. L. Davies, "Protein engineering of antifreeze proteins reveals that their activity scales with the area of the ice-binding site," *FEBS Lett.* **597**, 538–546 (2023).
- ⁶⁴K. Mochizuki and M. Matsumoto, "Collective transformation of water between hyperactive antifreeze proteins: RiAFPs," *Crystals* **9**, 188 (2019).